Electronic Supplementary Material (ESI) for Nanoscale.

Electronic Supplementary Information

Oxygen Vacancies-Rich Amorphous Porous NiFe$(OH)_x$ Derived from Ni$(OH)_x$/Prussian Blue as Highly Efficient Oxygen Evolution Electrocatalysts

Shuang Wang,[a] Xingbo Ge,*[a] Chao Lv,[b] Cun Hu,[b] Hongtai Guan,[a] Jing Wu,[a] Zhengnan Wang,[a] Xianhui Yang,[a] Yan Shi,[b] Jiangfeng Song,[b] Zhi Zhang,[b] Akira Watanabe [c] and Jinguang Cai *[b]

[a] School of Chemistry and Chemical Engineering, Southwest Petroleum University, Chengdu 610500, P. R. China

[b] Institute of Materials, China Academy of Engineering Physics, Jiangyou, 621908, Sichuan, P. R. China

[c] Institute of Multidisciplinary Research for Advanced Materials, Tohoku University, 2-1-1 Katahira, Aoba-ku, Sendai, 980-8577, Japan

*Corresponding authors: xbge@swpu.edu.cn; caijinguang@foxmail.com

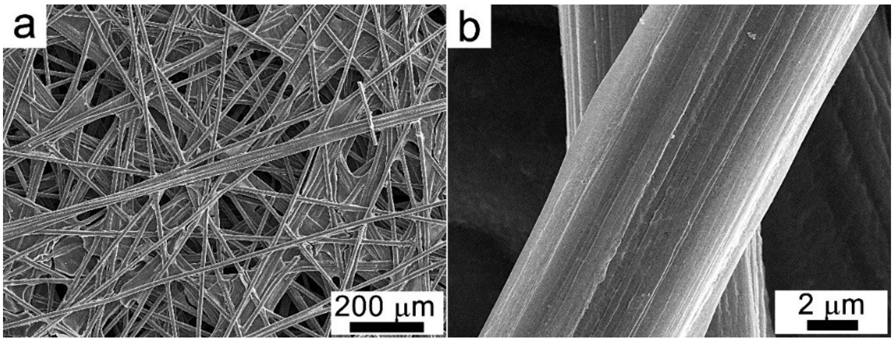

Fig. S1. SEM images (a, b) of a bare CP film.

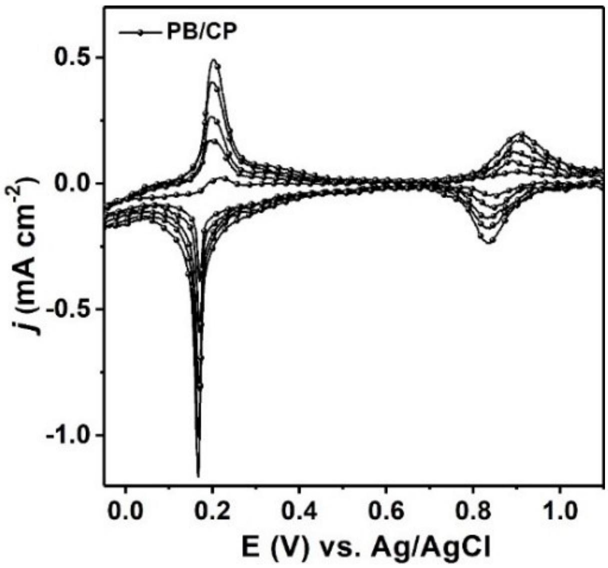

Fig. S2. CV curves for the electrodeposition of the PB layer on CP.

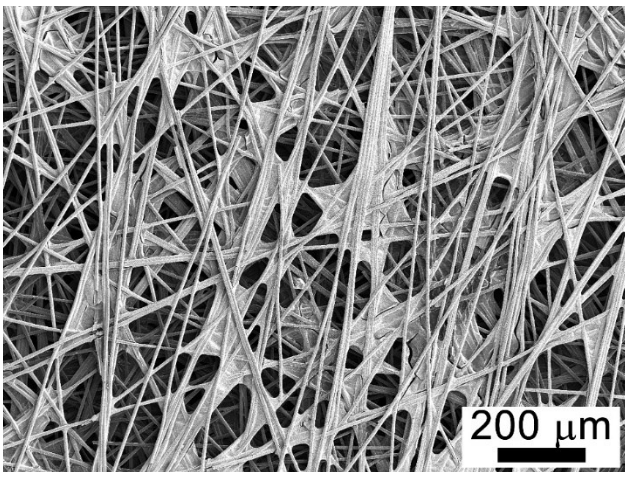

Fig. S3. Low-magnification SEM image of the PB/CP.

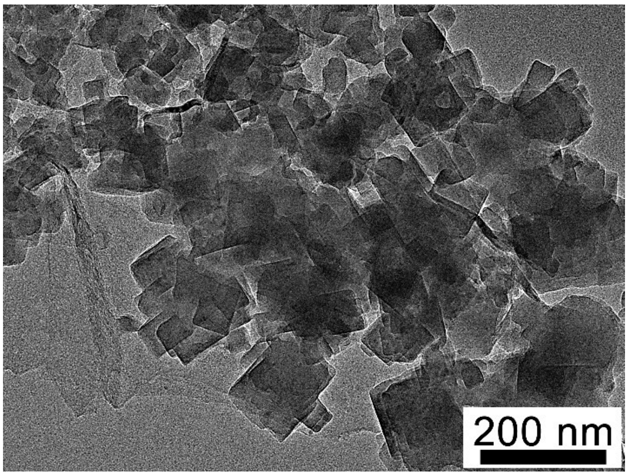

Fig. S4. TEM image of the PB nanoparticles peeling off from the carbon paper under strong ultrasonic.

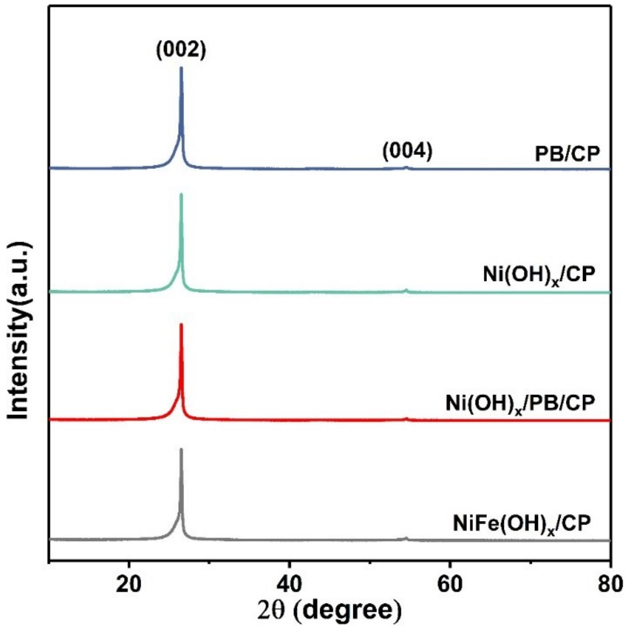

Fig. S5. XRD patterns of the PB/CP, $Ni(OH)_x$ /CP, $Ni(OH)_x$/PB/CP, and $NiFe(OH)_x$/CP.

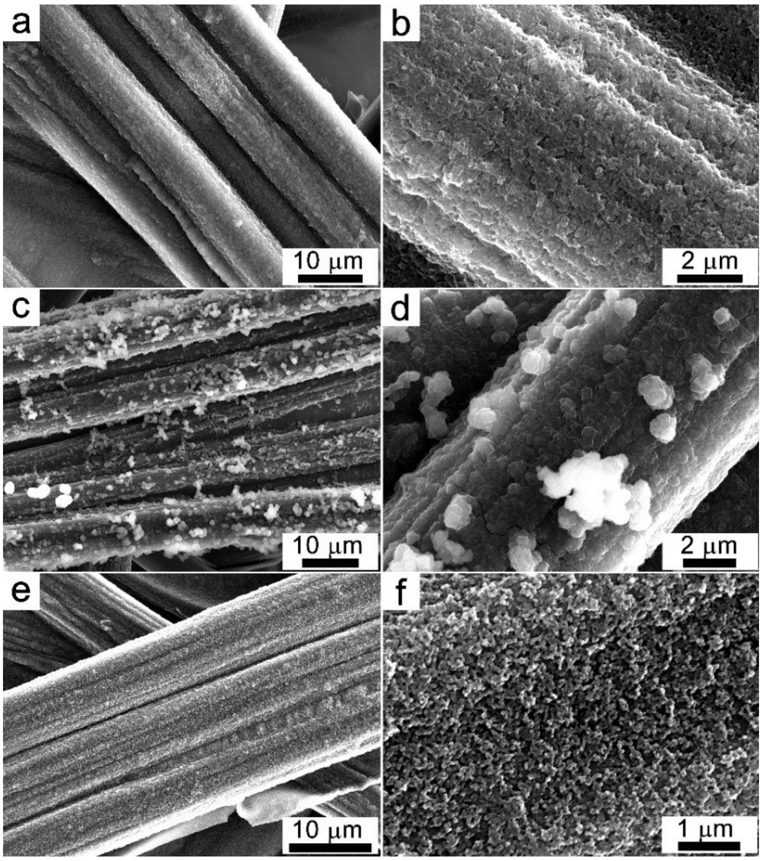

Fig. S6. SEM images of PB/CP samples obtained at different $Fe(NO_3)_3$ and $K_3[Fe(CN)_6]$ concentrations: 0.5 mM $Fe(NO_3)_3$ and 1 mM $K_3[Fe(CN)_6]$ (a, b), 1 mM $Fe(NO_3)_3$ and 0.5 mM $K_3[Fe(CN)_6]$ (c, d), and 2 mM $Fe(NO_3)_3$ and 0.5 mM $K_3[Fe(CN)_6]$ (e, f).

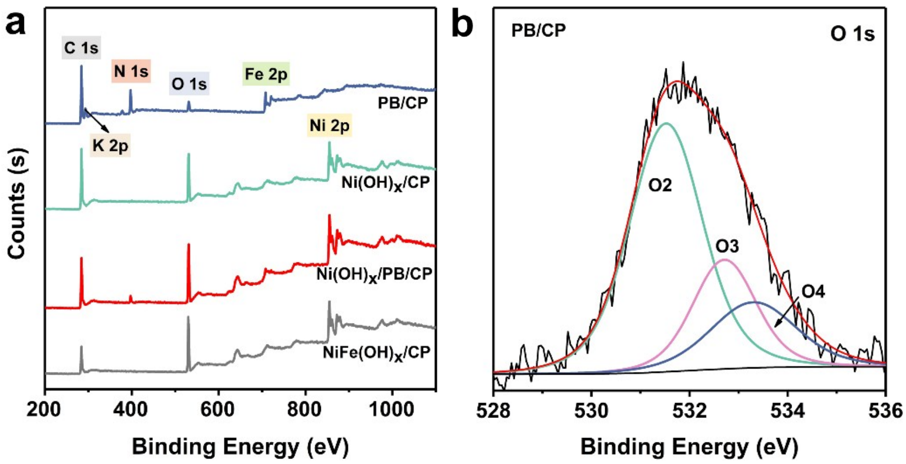

Fig. S7. Full XPS spectra of the PB/CP, $Ni(OH)_x/CP$, $Ni(OH)_x/PB/CP$, and $NiFe(OH)_x/CP$ (a) and high resolution O1s peak of the PB/CP (b).

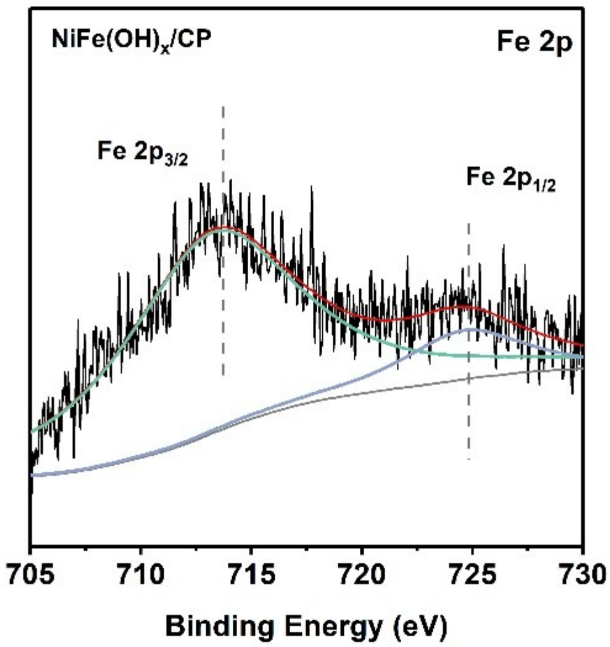

Fig. S8. Fe 2p XPS spectrum of the typical NiFe$(OH)_x$/CP.

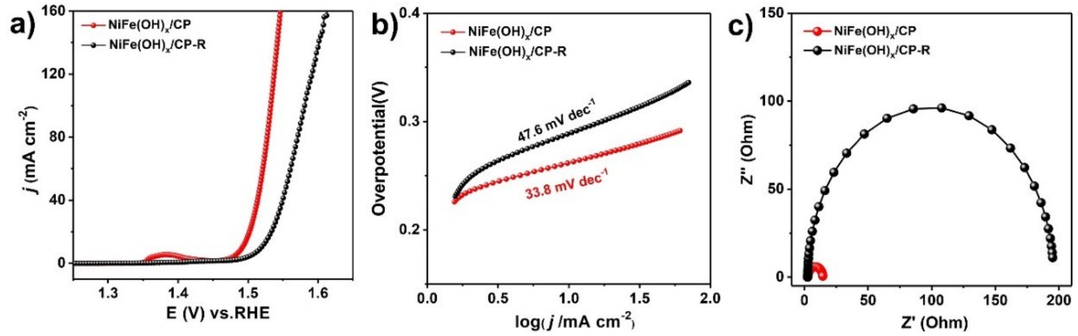

Fig. S9. iR-corrected polarization curves (a), corresponding Tafel plots (b), and EIS spectra (c) of the NiFe$(OH)_x$/CP and NiFe$(OH)_x$/CP-R.

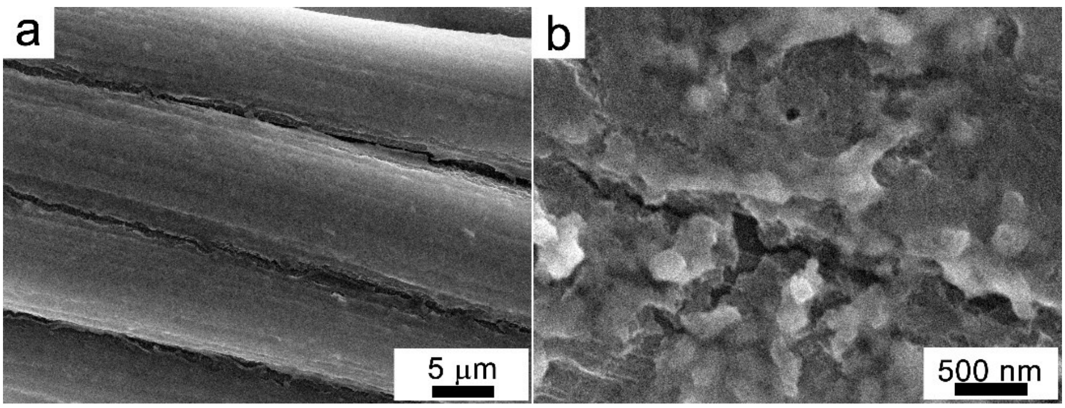

Fig. S10. Low- and high-magnification SEM images of the NiFe$(OH)_x$/CP after OER operation.

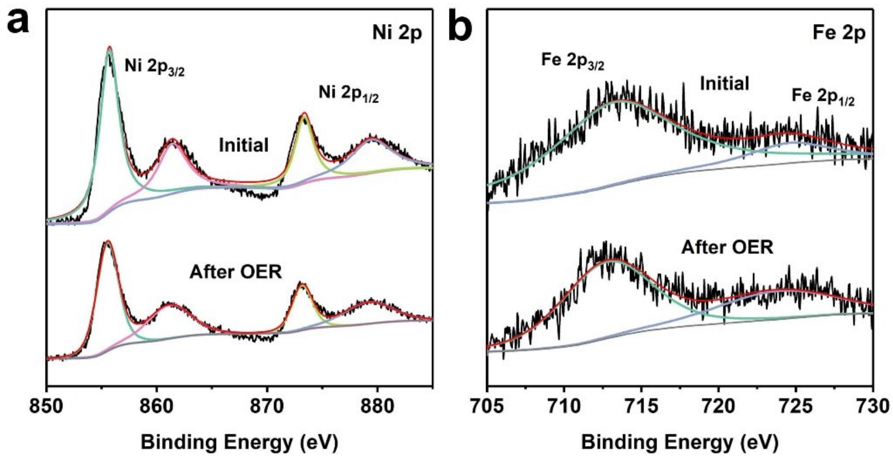

Fig. S11. XPS spectra of the $NiFe(OH)_x$/CP before and after OER operation: Ni 2p (a) and Fe 2p (b).

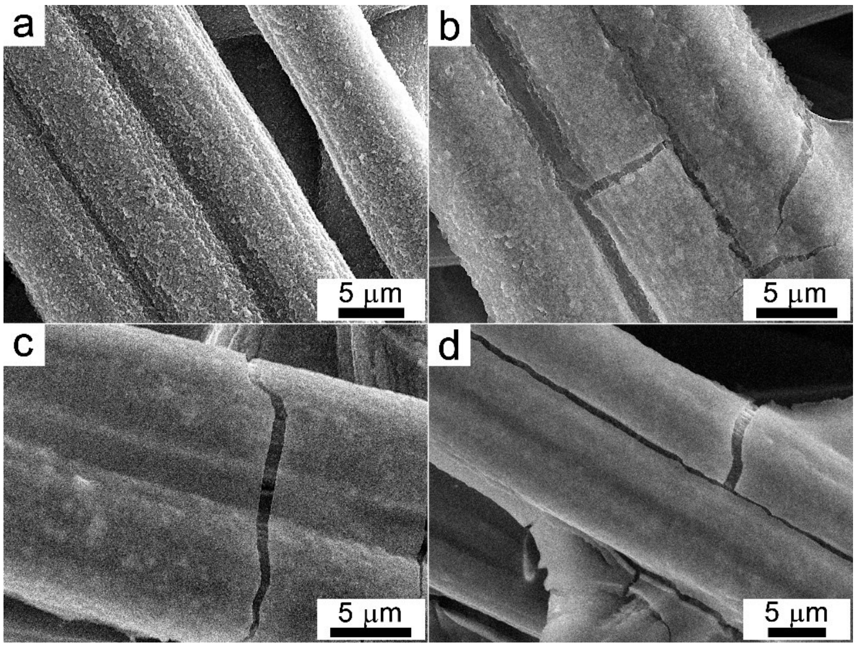

Fig. S12. SEM images of $Ni(OH)_x$/PB/CP obtained at different electrodeposition time of the $Ni(OH)_x$ layer in 1 mM $Ni(NO_3)_2$ solution: 60 s (a), 600 s (b), 2700 s (c), and 3600 s (d).

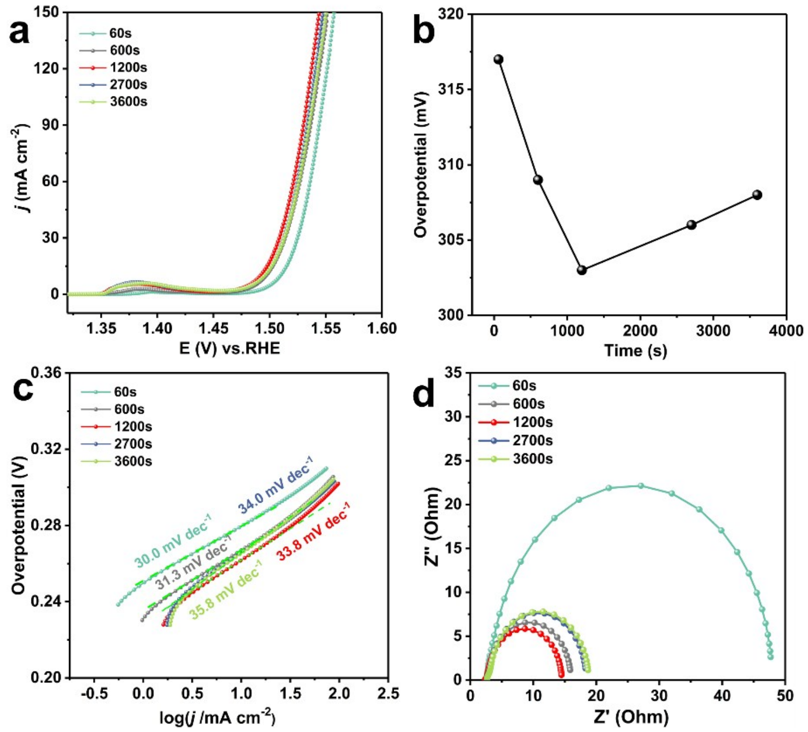

Fig. S13. LSV polarization curves (a), corresponding overpotentials at 100 mA cm^{-2} (b), Tafel slope plots (c), and EIS spectra (d) of the $Ni(OH)_x$/PB/CP prepared in 1 mM $Ni(NO_3)_2$ solution for different times.

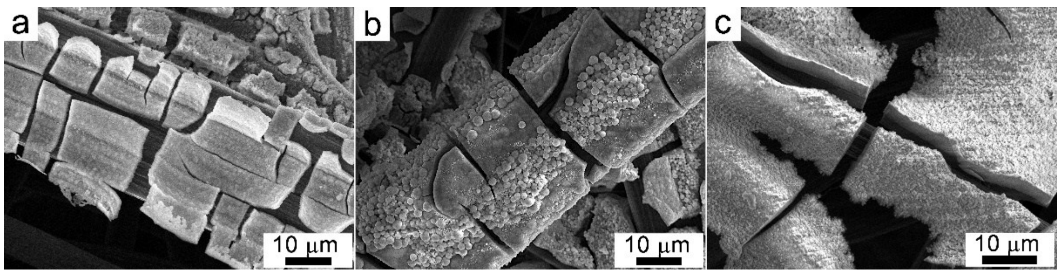

Fig. S14. SEM images of $Ni(OH)_x$/PB/CP prepared in $Ni(NO_3)_2$ solutions with different concentrations: 10 mM (a), 20 mM (b), and 50 mM (c).

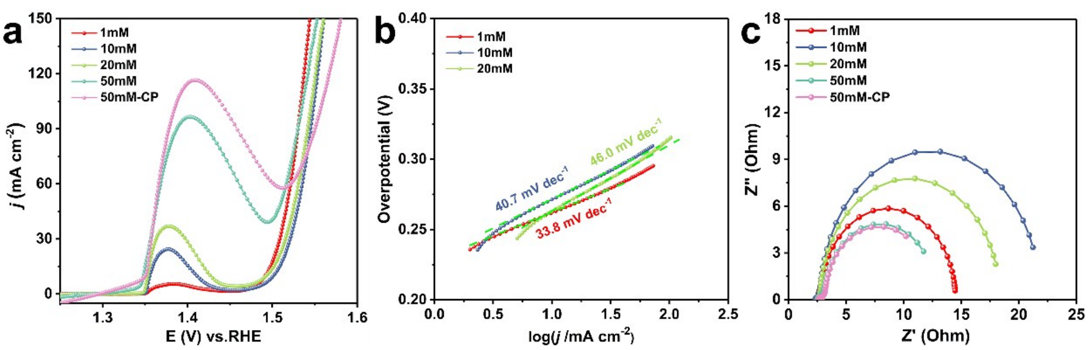

Fig. S15. LSV polarization curves (a), Tafel plots (b), and EIS spectra (c) for the $Ni(OH)_x$/PB/CP prepared in $Ni(NO_3)_2$ solutions with different concentrations.

Table S1. Concentrations of the electrolyte for electrochemical deposition of PB layer.

Sample	$Fe(NO_3)_3$ [mM]	$K_3[Fe(CN)_6]$ [mM]	KCl [M]	H_2SO_4 [mM]
a	0.5	0.5	0.1	12.5
b	0.5	1	0.1	12.5
c	1	0.5	0.1	12.5
d	2	0.5	0.1	12.5

Table S2. Summary on the OER performance of earth-abundant OER catalysts in 1.0 M KOH.

Catalysts [a)]	Loading amount [mg cm^{-2}]	Substrate	η@10 mA cm^{-2} [mV]	η@100 mA cm^{-2} [mV]	Tafel slope [mV dec^{-1}]	Stability test	Reference
Amorphous porous $NiFe(OH)_x$ layer	**~ 0.8**	**Carbon paper**	**261**	**303**	**33.8**	**50 h**	**This work**
Oxygen-enriched NiFe-LDH	0.28	Glassy carbon	310	_	74	9	1
NiFe LDH	1.03	Graphdiyne	260	_	95	6	2
NiFeOOH derived from NiFe PBA	0.25	Glassy carbon	258	304	46	_	3
Porous NiFe oxide nanocubes derived from NiFe PBA	2.2	Carbon fiber paper	271	_	48	18 h	4
NiFe oxyhydroxide derived from CN vacancy-mediated-PBA	0.255	Glassy carbon	283	_	54	25 h	5
FeNi LDH/Ti_3C_2 MXene	0.2	Ni foam	298	_	43	12	6
Phosphorylated NiFe hydroxide	–	Carbon fiber paper	290	_	38	10 h	7
N-doped carbon-coated core-shell $NiFeO_x$@NiFe phosphide derived from NiFe PBA/PVP	0.2	Glassy carbon	285	_	48	20 h	8
NiFeSe@NiSe|O derived from NiFe PBA	–	Carbon fiber	270	360	63.2	50 h	9
Plasma activated Co-PBA	2.0	Ni foam	274	330	53	_	10
Ni_3FeN nanoparticles/Reduced graphene oxide aerogel	0.5	Ni foam	270	_	54	10	11
$FeNi_3$ and $NiFe_2O_4$ embedded in N-doped carbon-carbon nanotube	0.5	Glassy carbon	274	_	_	11	12
Hybrid Ni-based MOFs nanosheets decorated	0.2	Glassy carbon	265	_	82	_	13

with Fe-MOF nanoparticles							
MOF-derived hierarchical $(Co,Ni)Se_2$@NiFe LDH hollow nanocages	–	Glassy carbon	277	–	75	17	14

[a] LDH: layered double hydroxide; PBA: Prussian blue analogue; PVP: polyvinylpyrrolidone; MOF: metal−organic framework.

Table S3. Molar ratio of Ni/Fe measured by ICP-OES for the $Ni(OH)_x$/PB/CP samples obtained at different deposition conditions of $Ni(OH)_x$ layer.

$Ni(NO_3)_2$ concentration [mM]	Deposition time [s]	Molar ratio of Ni/Fe
1	60	0.33
1	600	1.8
1	1200	1.9
1	2700	2.7
1	3600	3.4
10	1200	2.9
20	1200	36.25
50	1200	165.6

Reference

1 Chen, H.; Zhao, Q.; Gao, L.; Ran, J.; Hou, Y. Water-Plasma Assisted Synthesis of Oxygen-Enriched Ni–Fe Layered Double Hydroxide Nanosheets for Efficient Oxygen Evolution Reaction. *ACS Sustainable Chemistry & Engineering* **2019**, *7*, 4247-4254.

2 Shi, G.; Yu, C.; Fan, Z.; Li, J.; Yuan, M. Graphdiyne-Supported NiFe Layered Double Hydroxide Nanosheets as Functional Electrocatalysts for Oxygen Evolution. *ACS Applied Materials & Interfaces* **2019**, *11*, 2662-2669.

3 Su, X.; Wang, Y.; Zhou, J.; Gu, S.; Li, J.; Zhang, S. Operando Spectroscopic Identification of Active Sites in NiFe Prussian Blue Analogues as Electrocatalysts: Activation of Oxygen Atoms for Oxygen Evolution Reaction. *Journal of the American Chemical Society* **2018**, *140*, 11286-11292.

4 Kumar, A.; Bhattacharyya, S. Porous NiFe-oxide nanocubes as bifunctional electrocatalysts for efficient water-splitting. *ACS Applied Materials & Interfaces* **2017**, *9*, 41906-41915.

5 Yu, Z.-Y.; Duan, Y.; Liu, J.-D.; Chen, Y.; Liu, X.-K.; Liu, W.; Ma, T.; Li, Y.; Zheng, X.-S.; Yao, T.; Gao, M.-R.; Zhu, J.-F.; Ye, B.-J.; Yu, S.-H. Unconventional CN vacancies suppress iron-leaching in Prussian blue analogue pre-catalyst for boosted oxygen evolution catalysis. *Nature Communications* **2019**, *10*, 2799.

6 Yu, M.; Zhou, S.; Wang, Z.; Zhao, J.; Qiu, J. Boosting electrocatalytic oxygen evolution by synergistically coupling layered double hydroxide with MXene. *Nano Energy* **2018**, *44*, 181-190.

7 Li, Y.; Zhao, C. Enhancing Water Oxidation Catalysis on a Synergistic Phosphorylated NiFe Hydroxide by Adjusting Catalyst Wettability. *ACS Catalysis* **2017**, *7*, 2535-2541.
8 Hu, Q.; Liu, X.; Tang, C.; Fan, L.; Chai, X.; Zhang, Q.; Liu, J.; He, C. Facile fabrication of a 3D network composed of N-doped carbon-coated core–shell metal oxides/phosphides for highly efficient water splitting. *Sustainable Energy & Fuels* **2018**, *2*, 1085-1092.
9 Yilmaz, G.; Tan, C. F.; Lim, Y.-F.; Ho, G. W. Pseudomorphic Transformation of Interpenetrated Prussian Blue Analogs into Defective Nickel Iron Selenides for Enhanced Electrochemical and Photo-Electrochemical Water Splitting. *Advanced Energy Materials* **2019**, *9*, 1802983.
10 Guo, Y.; Wang, T.; Chen, J.; Zheng, J.; Li, X.; Ostrikov, K. Air Plasma Activation of Catalytic Sites in a Metal‐Cyanide Framework for Efficient Oxygen Evolution Reaction. *Advanced Energy Materials* **2018**, *8*, 1800085.
11 Gu, Y.; Chen, S.; Ren, J.; Jia, Y. A.; Chen, C.; Komarneni, S.; Yang, D.; Yao, X. Electronic Structure Tuning in Ni_3FeN/r-GO Aerogel toward Bifunctional Electrocatalyst for Overall Water Splitting. *ACS Nano* **2018**, *12*, 245-253.
12 Zhao, X.; Pachfule, P.; Li, S.; Simke, J. R. J.; Schmidt, J.; Thomas, A. Bifunctional Electrocatalysts for Overall Water Splitting from an Iron/Nickel‐Based Bimetallic Metal‐Organic Framework/Dicyandiamide Composite. *Angewandte Chemie International Edition* **2018**, *57*, 8921-8926.
13 Rui, K.; Zhao, G.; Chen, Y.; Lin, Y.; Zhou, Q.; Chen, J.; Zhu, J.; Sun, W.; Huang, W.; Dou, S. X. Hybrid 2D Dual-Metal–Organic Frameworks for Enhanced Water Oxidation Catalysis. *Advanced Functional Materials* **2018**, *28*, 1801554.
14 Li, J.-G.; Sun, H.; Lv, L.; Li, Z.; Ao, X.; Xu, C.; Li, Y.; Wang, C. Metal–Organic Framework-Derived Hierarchical (Co,Ni)Se_2@NiFe LDH Hollow Nanocages for Enhanced Oxygen Evolution. *ACS Applied Materials & Interfaces* **2019**, *11*, 8106-8114.